

Site-mixing effect on the XMCD spectrum in double perovskite $\text{Bi}_2\text{FeMnO}_6$

Cite as: Appl. Phys. Lett. **108**, 242907 (2016); <https://doi.org/10.1063/1.4953828>
Submitted: 29 March 2016 . Accepted: 01 June 2016 . Published Online: 15 June 2016

Towfiq Ahmed, Aiping Chen, Brian McFarland, Qiang Wang, Hendrik Ohldag, Richard Sandberg, Quanxi Jia, Dmitry A. Yarotski, and Jian-Xin Zhu



View Online



Export Citation



CrossMark

ARTICLES YOU MAY BE INTERESTED IN

[Magnetic, electronic, and optical properties of double perovskite \$\text{Bi}_2\text{FeMnO}_6\$](#)
APL Materials **5**, 035601 (2017); <https://doi.org/10.1063/1.4964676>

[Magnetic properties of \$\text{Bi}_2\text{FeMnO}_6\$: A multiferroic material with double-perovskite structure](#)
Applied Physics Letters **97**, 122502 (2010); <https://doi.org/10.1063/1.3490221>

[Anisotropy of crystal growth mechanisms, dielectricity, and magnetism of multiferroic \$\text{Bi}_2\text{FeMnO}_6\$ thin films](#)
Journal of Applied Physics **113**, 17D904 (2013); <https://doi.org/10.1063/1.4794724>

Applied Physics Letters

Mid-IR and THz frequency combs
special collection

[Read Now!](#)

AIP
Publishing

Site-mixing effect on the XMCD spectrum in double perovskite $\text{Bi}_2\text{FeMnO}_6$

Towfiq Ahmed,^{1,a)} Aiping Chen,² Brian McFarland,² Qiang Wang,³ Hendrik Ohldag,⁴ Richard Sandberg,² Quanxi Jia,² Dmitry A. Yarotski,^{2,b)} and Jian-Xin Zhu^{1,2,c)}

¹Theoretical Division, Los Alamos National Laboratory, Los Alamos, New Mexico 87545, USA

²Center for Integrated Nanotechnologies, Los Alamos National Laboratory, Los Alamos, New Mexico 87545, USA

³Material Science Division, Argonne National Laboratory, Lemond, Illinois 60439, USA

⁴Stanford Synchrotron Radiation Laboratory, Mailstop 69, Menlo Park, California 94025, USA

(Received 29 March 2016; accepted 1 June 2016; published online 15 June 2016)

We investigate magnetization in double perovskite multiferroic $\text{Bi}_2\text{FeMnO}_6$ (BFMO) thin film using density functional theory (DFT) simulations, and X-ray magnetic circular dichroism (XMCD) measurements. The exchange interaction between Fe and Mn sites gives rise to a ferrimagnetic ordering in BFMO. When grown without structural defects, distinct XMCD signal is expected from this system. The site resolved magnetization, thus, can be extracted using XMCD sum rules. Although our theoretical calculations are consistent with this expectation for the ideal BFMO system, experimental measurements find evidence of anomalous peak for the L_2 and L_3 edges of XMCD signals, and thus, the XMCD sum rules are no longer valid. We theoretically explain this phenomenon by considering both tetragonal (near interface), and monoclinic (bulk) phases of BFMO system, with Fe and Mn ions interchanged between their respective sites. Such site-mixing between magnetic cations are commonly found during the synthesis process. Our DFT calculations of XMCD for site interchanged Fe and Mn ions in the bulk phase (monoclinic) of BFMO are in good agreement with experimental XMCD signal and reproduce the anomalous peak features at L_2/L_3 edges. *Published by AIP Publishing.* [<http://dx.doi.org/10.1063/1.4953828>]

In the ongoing search for multiferroics with coexisting ferromagnetism and ferroelectricity at room temperature (RT), the ordered double perovskite systems have recently attracted much interest from the condensed matter and materials science community. Although several potential single perovskite multiferroics have been synthesized experimentally, quite often they have limited applications by having either a very low Curie temperature (T_c) for ferromagnetic order¹ or a high Neel temperature (T_N) but almost zero net magnetization.² Two of the most recent yet widely studied single perovskite multiferroics are BiFeO_3 (BFO) and BiMnO_3 (BMO). Stoichiometrically active lone pair $6s^2$ electrons are responsible for the displacement of Bi atoms in both systems which causes ferroelectric ordering at RT with $T_c = 1103$ K and 760 K in BFO and BMO, correspondingly. However, BFO is antiferromagnetic (AFM) with $T_N = 643$ K while BMO is a very low temperature ferromagnet ($T_c = 110$ K). Due to these caveats for having ferroelectricity with net magnetic moment in single perovskite systems, there has been active effort by many groups worldwide to design heterostructure or double perovskite systems, which are multiferroic at RT.

To achieve this goal, our effort in this work is directed towards synthesis, characterization, and theoretical simulations of double perovskite $\text{Bi}_2\text{FeMnO}_6$ (BFMO), a potential RT multiferroic system. While the ferroelectric behavior in BFMO should be robust due to the $6s^2$ lone-pair electrons in Bi ions, an insulating ferrimagnetic phase can emerge due to the dominant ferromagnetic Hund coupling on the adjacent

Fe and Mn ions. This can be understood by following Goodenough-Kanamori (GK) rules in a typical rock-salt configuration.³ Within the GK rule, no super exchange interaction mediated by oxygen in between Fe and Mn ions is necessary, and thus, BFMO can become a ferroelectric insulator with net ferrimagnetic moment even at room temperature.

Considering BFMO as a potential candidate for RT-multiferroics, we synthesized BFMO through the dilution of Fe-sublattice by Mn in BFO, while the end member BMO is isostructural to BiFeO_3 . Recently, the measurements on strained thin BFMO films (thickness ~ 30 nm)⁴ have shown a large magnetic moment of $\sim 1.16 \mu_B/\text{f.u.}$ at room temperature, while only a small magnetic moment of less than $0.01 \mu_B/\text{f.u.}$ at 5 K was observed for thicker films (thickness ~ 220 nm). The significant difference of the magnetic moments in thin and thick films originates from the fact that the much thinner thin films are highly strained and have a tetragonal crystal structure (Fig. 1(a)), while the thick films are more relaxed and monoclinic (Fig. 1(c))—suggesting the importance of strain effect on the magnetism of BFMO. Experimentally,⁴ it was found that the SrTiO_3 (STO) substrate modifies the unit cell parameters of BFMO thin films, and the cubic perovskite structure takes a coherent tetragonal form with 2.5% increase in c parameters. Theoretically, the first-principles simulations have been carried out for the thick films and the full relaxation of the atomic coordinates and lattice parameters leads to the most stable monoclinic structure without a magnetic ordering.⁵

In order to understand and illustrate the magnetic property in BFMO, we have performed the X-ray magnetic circular dichroism (XMCD) measurements in our synthesized thin

^{a)}atowfiq@lanl.gov

^{b)}dzmitry@lanl.gov

^{c)}jxzhou@lanl.gov. URL: <http://cint.lanl.gov>

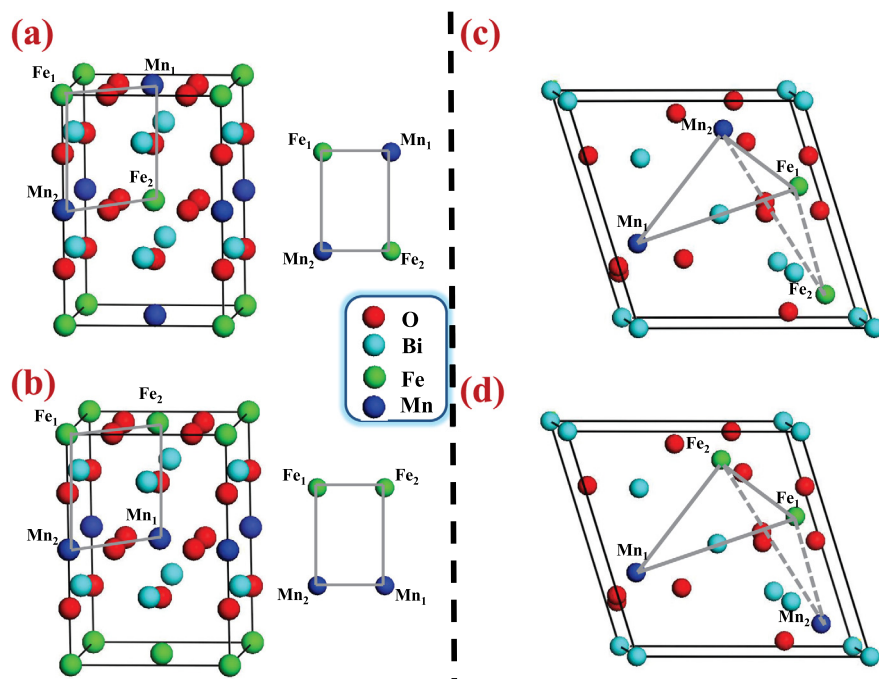


FIG. 1. Crystal structure of the double perovskite BFMO: (a) regular tetragonal unit cell and Fe-Mn plane shown in rectangular plaquette; (b) site-mixed (between Mn₁ and Fe₂) tetragonal unit cell; (c) regular (unmixed) monoclinic unit cell; and (d) site-mixed (between Mn₂ and Fe₂) monoclinic unit cell.

film with ~ 30 nm thickness. Although initially it was believed that XMCD spectroscopy will capture interfacial magnetic behavior in BFMO, the XMCD spectral features at Fe and Mn L_2/L_3 edges showed unexpectedly a scenario far from ferromagnetic ordering in transition-metal ions. Both Fe and Mn L_2 and L_3 edges exhibit an interference of shifted resonances in the XMCD signal, where a net magnetization is very small and sum rules are no longer applicable.

The primary suspect for the cause of such XMCD peak behavior is site-mixing—either originating from mixed valence in Mn and Fe, or site exchange between Fe and Mn ions. Either case is possible particularly when the BFMO system possesses lower symmetry (monoclinic) structure as often found in the bulk. In monoclinic BFMO, chemical environment is distinguishable for Mn and Fe ion sites (Fig. 1(c)), and can cause core-level shifts which affect the X-ray absorption spectra (XAS). Since the attenuation length of the total electron yield (TEY) signal in insulating perovskite oxides is usually not more than a few nanometers,⁶ the XMCD signal we measured is dominated by the bulk-like BFMO phase near the surface of the sample. Our experimentally observed XMCD signals are thus coming from the bulk-like layers in thin film BFMO, and the oscillating W-shaped peak features can be understood by considering a very simple site-mixing scenario. In this work, we performed density functional theory (DFT) calculations of L_2/L_3 edge XMCD spectra of Fe and Mn ions for both tetragonal (modeling those layers near STO interface) and monoclinic (modeling those bulk-like layers near surface) phases. Considering site-mixing between Fe and Mn ions for both structural phases, we demonstrate the physical origin of oscillatory XMCD spectra found in our measurements. Although a possible alternative scenario is the existence of mixed valence cations (Mn³⁺/Mn⁴⁺ and Fe²⁺/Fe³⁺), which are sometimes considered to cause W-shaped XMCD signals, they predominantly exist in more complex molecular-solid like systems with Mn and Fe ions,^{7–9} and γ -Fe₂O₃.¹⁰ However, mixed-valence cations, despite of

W-shaped XMCD signal, will still lead to net magnetic moment with significant ferri- or ferromagnetic ordering, in contrast with our experimental findings in bulk BFMO with vanishing magnetic moment. On the other hand, our theoretical explanation based on site-mixing between Fe and Mn in monoclinic BFMO is more suitable for solid perovskite systems. It was found earlier that in both BMO and BFMO, Mn stays at 3+ valence state.⁵ Furthermore, the site-mixing scenario also explains the smaller net magnetic moment found in the bulk BFMO with monoclinic symmetry. Experimentally, such a site-mixing happens during the synthesis process, and was earlier observed in other double perovskite systems, e.g., Lu₂MnCoO₆.¹¹

Bi₂FeMnO₆ films were grown on SrTiO₃ (STO) (001) substrates by pulsed laser deposition with a KrF laser (248 nm). The Bi₂FeMnO₆ target was prepared by mixing stoichiometric amounts of high purity (99.99%) Bi₂O₃, Fe₂O₃, and MnO₂, with a sintering temperature of 800 °C. A substrate temperature of 680 °C and an oxygen pressure of 100 mTorr were maintained during depositions. The rectangular laser beam with an area of 5.55 mm² was focused onto the target with an energy density of 1.5 J/cm². After deposition, films were cooled down to room temperature in an oxygen pressure of 250 Torr. The XMCD signals were measured in a total electron yield (TEY) geometry using Dichroism Soft X-ray Spectroscopy Beamline 13-1 at the Stanford Synchrotron Radiation Light Source. Elliptical polarizing undulator produces left- and right circularly polarized X-ray photons in a 500–1200 eV range that encompasses magnetically sensitive L_2/L_3 resonances of Fe and Mn elements. Prior to the measurements, the samples were attached to the copper cryostat cold finger with carbon tape and then cooled down to 10 K in the magnetic field of 0.25 T oriented in the sample surface plane. The field was then switched off, and the sample was rotated so that the X-ray beam was incident at a 30° angle to the surface plane. X-ray absorption for both circular polarizations were acquired at a temperature

$T = 10$ K over an energy range of 625–670 eV for Mn and 690–740 eV for Fe L3 and L2 edges, respectively. To study the electronic and magnetic properties of double perovskite $\text{Bi}_2\text{FeMnO}_6$, we applied DFT as implemented in the full-potential LAPW code WIEN2k.¹² The tetragonal crystal structure of BFMO is shown in Fig. 1(a). For the same symmetry, site-mixing (between Mn_1 and Fe_2) crystal structure is shown in Fig. 1(b). All Fe and Mn ions are co-planar in the tetragonal BFMO, and shown by the rectangular plaquette next to the conventional unit cell. The most stable structure is monoclinic (C_2 symmetry)⁵ in bulk BFMO, and is shown in Fig. 1(c). The site-interchanged structure (between Fe_2 and Mn_2) is shown in Fig. 1(d). For all these four cases, we calculated L_2/L_3 edge XMCD for Mn_1 , Mn_2 , Fe_1 , and Fe_2 ions. The details of our computational method and used parameters are provided in the supplementary material.¹³

To understand the vanishing magnetization in bulk BFMO with monoclinic unit cell, and its relation to the oscillatory peak features in L_2/L_3 edge XMCD spectra, we self-consistently calculated the magnetic moments and XMCD of Mn and Fe ions for both tetragonal and monoclinic structural phases. We first investigate tetragonal BFMO, which is most stable near STO interface. We doubled the unit cell to have two Mn and two Fe ions, and identified them as Mn_1 , Mn_2 , Fe_1 , and Fe_2 . Results for regular tetragonal structure (no mixing between Fe and Mn ions) are shown in Figs. 2(a) and 2(b). Similarly, Figs. 2(c) and 2(d) show the XMCD spectra for the doubled unit cell with site-mixing between Mn_1 and Fe_2 ions. This can also be geometrically realized by comparing the top and bottom rectangular plaquette of Mn-Fe planes as in Fig. 2. In the regular tetragonal phase, Mn_1 and Mn_2 sites are found indistinguishable in our DFT calculations, each having magnetic moment $-3.09 \mu_B$. Similarly, the Fe_1 or Fe_2 has magnetic moment $+3.64 \mu_B$. In Fig. 2(a), the left (green curve) and right (red curve) circularly polarized XAS for L_2 and L_3 edges of Mn and Fe ions are shown. The difference

between left and right circularly polarized XAS is defined as an XMCD signal, which is shown as the black curves for Mn and Fe ions. Due to the higher crystal symmetry of the tetragonal structure, the chemical environments around the Mn sites or the Fe sites are precisely identical, and thus no chemical shift of the core levels is observed between Mn_1 and Mn_2 ions. Same is true for Fe_1 and Fe_2 ions. Therefore, for the Mn or Fe sites, the averaged XMCD spectra contain distinct peak features, as shown in Fig. 2(b). On the other hand, when the Fe and Mn ions are interchanged in the unit cell, each Fe and Mn sublattice becomes AFM ordered with equal and opposite magnetic moments. Therefore, the averaged XMCD spectra for Fe_1 and Fe_2 , or equivalently Mn_1 and Mn_2 , show almost flat lines without any distinct or oscillatory peak features (Fig. 2(d)). Since such an outcome is not consistent with our experimental finding, we need to analyze XMCD spectra for the monoclinic unit cell of BFMO near the bulk like layers of the BFMO thin film.

In the relaxed bulk BFMO, the monoclinic structure with C_2 symmetry was earlier found to be more stable.⁵ Due to lower symmetry structure, the unit cell of near the surface of BFMO film may contain two distinct Mn ions (Mn_1 and Mn_2) and Fe ions (Fe_1 and Fe_2) embedded in different local chemical environment. To investigate such local effect on the magnetism in bulk BFMO, we self-consistently calculated the magnetic moments in both regular (Fig. 3(a)) and site-mixed (Fig. 3(b)) BFMO unit cell. The four cations (two Mn and two Fe) are not in a same plane, as shown by the two triangles in the insets of Figs. 3(a) and 3(b). In the regular monoclinic unit cell (Fig. 3(a)), our DFT calculations predict XMCD spectra with expected distinct peak features with negligible chemical shift observed among Mn_1 , Mn_2 , Fe_1 , and Fe_2 ions. The self-consistently calculated average magnetic moments for Mn and Fe ions are $-2.946 \mu_B$ and $3.26 \mu_B$, correspondingly.

Our experimental measurements of L_2/L_3 edge XMCD signals at 10 K (the bottom curves in Fig. 3(b)), display unexpected W-shaped features. To explain this, we

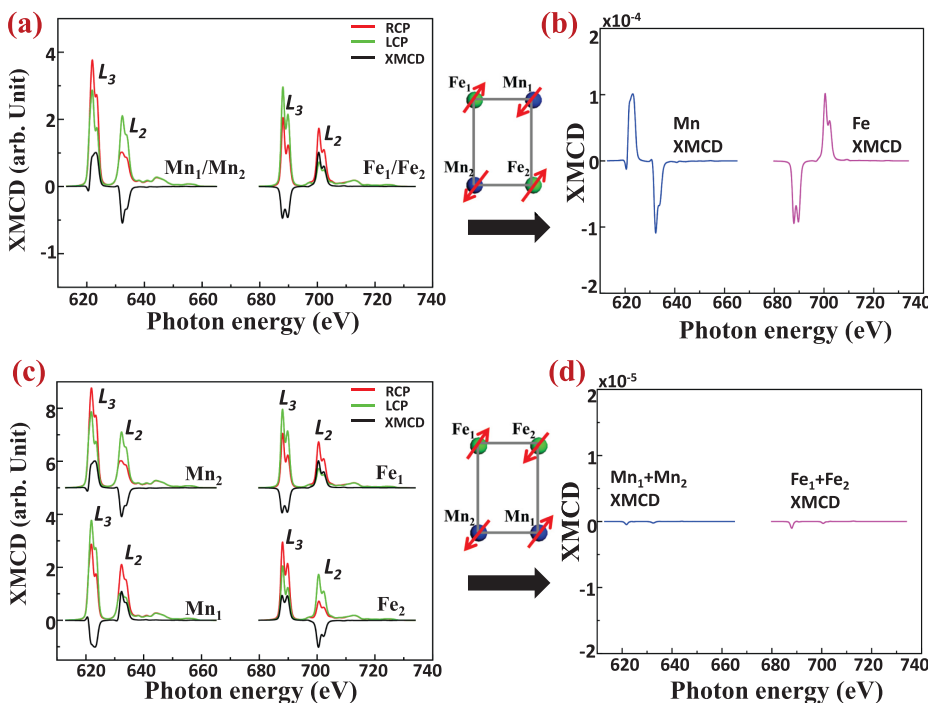


FIG. 2. Calculated XMCD in regular unmixed case ((a) and (b) panels) and site-mixed tetragonal ((c) and (d) panels) unit cells in BFMO. Red and green curves in (a) and (b) are right and left circularly polarized XAS, respectively. Magnetic ordering in Fe and Mn sites are shown in the rectangular plaquettes, where the Fe and Mn sublattices are antiferromagnetically aligned for the site-mixed case (panels (c) and (d)). Site averaged XMCD for Mn and Fe sublattices are shown in (b) for regular case and in (d) for site-mixed case.

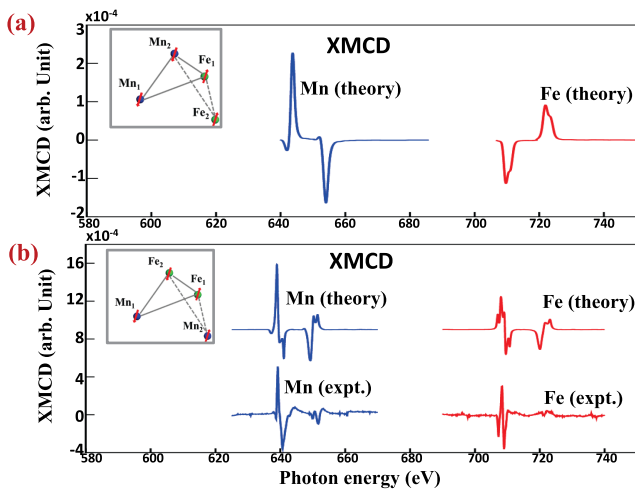


FIG. 3. L_2/L_3 edge XMCD of Mn and Fe sites in BFMO for the monoclinic unit cell. Panel (a) is for regular unmixed case, and panel (b) is for site-mixed (between Mn_2 and Fe_2) case. Mn and Fe sublattices are in two different planes shown by triangles in (a) and (b) insets. For the unmixed regular structure, calculated XMCD for Mn (blue) and Fe (red) shown in (a), while for the site-mixed case both experimental and calculated XMCD spectra for Mn (blue) and Fe (red) are shown in (d).

considered the site mixing between Mn_2 and Fe_2 , as shown in the inset of Fig. 3(b). Our DFT calculated XMCD spectra are the top curves in Fig. 3(b). It is clear that the oscillatory peak features are reproduced and are in good agreement with experimental observation. The agreement between theory and experiment strongly suggests that, during the sample growth process on STO substrate, the Fe and Mn ions are site mixed near the surface region accompanying the structural change from the tetragonal to monoclinic phase. Similar mixing was also observed earlier for other double perovskite systems. The site-mixing in Lu_2MnCoO_6 crystal as determined by neutron scattering experiment is about 9% throughout the entire bulk.¹¹ Since the difference of the atomic radius between Mn ($r_{at} = 1.61 \text{ \AA}$), and Fe ($r_{at} = 1.56 \text{ \AA}$) is smaller than that between Mn and Co ($r_{at} = 1.52 \text{ \AA}$), the site-mixing rate in BFMO bulk should be slightly higher than in Lu_2MnCoO_6 . More importantly, in the BFMO thin-film sample, although an accurate estimate of the amount of site-mixing is unavailable, from the comparison of the theoretical results with the species-sensitive XMCD spectroscopy and magnetization measurement,^{4,14} we are still able to propose that the site-mixing at the top few layers of BFMO should be much stronger than in those close to the substrate. This heterogeneity could also be related to the structure evolution throughout the thin film.

We have studied the effects of Fe and Mn site mixing on the XMCD spectra in the double perovskite BFMO thin film through the DFT band structure calculations closely coupled to the XMCD measurements. Although significant ferrimagnetic ordering was earlier observed in magnetic hysteresis experiments performed on the thin films of BFMO grown on STO,¹⁵ our XMCD measurements on $\sim 30 \text{ nm}$ film of BFMO has detected unexpected W-shape features with vanishing

magnetization. In view of the fact that the detection of the total electron yield of L_2 and L_3 edges x-ray absorption spectra has 2–3 nm attenuation length, and thus can only probe a few nanometers near the surface, we have proposed that these few nanometers region has already recovered the monoclinic structure typically present in bulk BFMO and the commonly found site-mixing between Mn and Fe ions during the synthesis process can create antiferromagnetically ordered Mn and Fe sublattices. Together with the core-level shift in ions within the Mn and Fe sublattices, which is caused by different local chemical environments in the monoclinic structure, our first-principles calculations of site averaged XMCD for Mn and Fe L_2/L_3 edges can explain the experimental XMCD.

We thank Sven Rudin and Vivian Zapf for useful discussions. This work was supported by the U.S. DOE at LANL under Contract No. DE-AC52-06NA25396 through the LANL LDRD Program. Use of the Stanford Synchrotron Radiation Light Source, SLAC National Accelerator Laboratory, was supported by the U.S. DOE BES under Contract No. DE-AC02-76SF00515. The work was in part supported by the Center for Integrated Nanotechnologies, a U.S. DOE BES user facility.

¹A. M. dos Santos, S. Parashar, A. Raju, Y. Zhao, A. Cheetham, and C. Rao, *Solid State Commun.* **122**, 49 (2002), ISSN: 0038-1098.

²J. R. Teague, R. Gerson, and W. James, *Solid State Commun.* **8**, 1073 (1970), ISSN: 0038-1098.

³M. Azuma, K. Takata, T. Saito, S. Ishiwata, Y. Shimakawa, and M. Takano, *J. Am. Chem. Soc.* **127**, 8889 (2005).

⁴E.-M. Choi, S. Patnaik, E. Weal, S.-L. Sahonta, H. Wang, Z. Bi, J. Xiong, M. G. Blamire, Q. X. Jia, and J. L. MacManus-Driscoll, *Appl. Phys. Lett.* **98**, 012509 (2011).

⁵L. Bi, A. R. Taussig, H.-S. Kim, L. Wang, G. F. Dionne, D. Bono, K. Persson, G. Ceder, and C. A. Ross, *Phys. Rev. B* **78**, 104106 (2008).

⁶A. Ruosi, C. Raisch, A. Verna, R. Werner, B. A. Davidson, J. Fujii, R. Kleiner, and D. Koelle, *Phys. Rev. B* **90**, 125120 (2014).

⁷G. Peng, J. van Elp, H. Jang, L. Que, Jr., W. H. Armstrong, and S. P. Cramer, *J. Am. Chem. Soc.* **117**, 2515 (1995).

⁸G. Subías, J. García, and M. C. Sánchez, *AIP Conf. Proc.* **882**, 783 (2007).

⁹M. M. Grush, J. Chen, T. L. Stemmler, S. J. George, C. Y. Ralston, R. T. Stibrany, A. Gelasco, G. Christou, S. M. Gorun, J. E. Penner-Hahn *et al.*, *J. Am. Chem. Soc.* **118**, 65 (1996).

¹⁰R. Grau-Crespo, A. Y. Al-Baitai, I. Saadoune, and N. H. D. Leeuw, *J. Phys.: Condens. Matter* **22**, 255401 (2010).

¹¹S. Yáñez Vilar, E. D. Mun, V. S. Zapf, B. G. Ueland, J. S. Gardner, J. D. Thompson, J. Singleton, M. Sánchez-Andújar, J. Mira, N. Biskup *et al.*, *Phys. Rev. B* **84**, 134427 (2011).

¹²P. Blaha, K. Schwarz, G. K. H. Madsen, D. Kvasnicka, and J. Luitz, *An Augmented Plane Wave + Local Orbitals Program for Calculating Crystal Properties* (Karlheinz Schwarz, Tech. Universität Wien, Austria, 2001).

¹³See supplementary material at <http://dx.doi.org/10.1063/1.4953828> for details of the computational method.

¹⁴E.-M. Choi, T. Fix, A. Kursumovic, C. J. Kinane, D. Arena, S.-L. Sahonta, Z. Bi, J. Xiong, L. Yan, J.-S. Lee, H. Wang, S. Langridge, Y.-M. Kim, A. Y. Borisevich, I. MacLaren, Q. M. Ramasse, M. G. Blamire, Q. Jia, and J. L. MacManus-Driscoll, *Adv. Funct. Mater.* **24**(47), 7478–7487 (2014).

¹⁵T. Ahmed, A. Chen, D. A. Yarotski, S. A. Trugman, Q. Jia, and J.-X. Zhu, “Magnetic, Electronic and Optical Properties of Double Perovskite Bi_2FeMnO_6 ” (unpublished).